

Thermal conductivity of GeTe crystals based on machine learning potentials

Jian Zhang(张健), Hao-Chun Zhang(张昊春), Weifeng Li(李伟峰), and Gang Zhang(张刚)

Citation: Chin. Phys. B, 2024, 33 (**4**): 047402. DOI: 10.1088/1674-1056/ad1b42
Journal homepage: http://cpb.iphy.ac.cn; http://iopscience.iop.org/cpb

What follows is a list of articles you may be interested in

Ultralow-temperature heat transport study of noncentrosymmetric superconductor CaPtAs

Yimin Wan(万一民), Erjian Cheng(程二建), Yuxin Chen(陈宇鑫), Chengcheng Zhao(赵成成), Chengpeng Tu(涂成鹏), Dongzhe Dai(戴东喆), Xiaofan Yang(杨小帆), Lu Xin(辛路), Wu Xie(谢武), Huiqiu Yuan(袁辉球), and Shiyan Li(李世燕)

Chin. Phys. B, 2023, 32 (**12**): 127403. DOI: 10.1088/1674-1056/ad02e9

Advances in thermoelectric $(GeTe)_x(AgSbTe_2)_{100-x}$

Hongxia Liu(刘虹霞), Xinyue Zhang(张馨月), Wen Li(李文), and Yanzhong Pei(裴艳中)

Chin. Phys. B, 2022, 31 (**4**): 047401. DOI: 10.1088/1674-1056/ac3cae

Two-dimensional square-Au_2S monolayer: A promising thermoelectric material with ultralow lattice thermal conductivity and high power factor

Wei Zhang(张伟), Xiao-Qiang Zhang(张晓强), Lei Liu(刘蕾), Zhao-Qi Wang(王朝棋), and Zhi-Guo Li(李治国)

Chin. Phys. B, 2021, 30 (**7**): 077405. DOI: 10.1088/1674-1056/abe115

Fabrication and characterization of Al-Mn superconducting films for applications in TES bolometers

Qing Yu(余晴), Yi-Fei Zhang(张翼飞), Chang-Hao Zhao(赵昌昊), Kai-Yong He(何楷泳), Ru-Tian Huang(黄汝田), Yong-Cheng He(何永成), Xin-Yu Wu(吴歆宇), Jian-She Liu(刘建设), and Wei Chen(陈炜)

Chin. Phys. B, 2021, 30 (**7**): 077402. DOI: 10.1088/1674-1056/abe0c6

Thermal stability and thermoelectric properties of Cd-doped nano-layered Cu_2Se prepared using NaCl flux method

Jianhua Lu(陆建华), Decong Li(李德聪), Wenting Liu(刘文婷), Lanxian Shen(申兰先), Jiali Chen(陈家莉), Wen Ge(葛文), and Shukang Deng(邓书康)

Chin. Phys. B, 2020, 29 (**12**): 127403. DOI: 10.1088/1674-1056/abbbf5

SPECIAL TOPIC — Heat conduction and its related interdisciplinary areas

Thermal conductivity of GeTe crystals based on machine learning potentials

Jian Zhang(张健)[1,2], Hao-Chun Zhang(张昊春)[1,†], Weifeng Li(李伟峰)[3], and Gang Zhang(张刚)[2,‡]

[1] *School of Energy Science and Engineering, Harbin Institute of Technology, Harbin* 150001, *China*
[2] *Institute of High Performance Computing, Agency for Science, Technology and Research (A*STAR), Singapore* 138632, *Singapore*
[3] *School of Physics & State Key Laboratory of Crystal Materials, Shandong University, Jinan* 250100, *China*

(Received 13 November 2023; revised manuscript received 23 December 2023; accepted manuscript online 5 January 2024)

GeTe has attracted extensive research interest for thermoelectric applications. In this paper, we first train a neuro-evolution potential (NEP) based on a dataset constructed by *ab initio* molecular dynamics, with the Gaussian approximation potential (GAP) as a reference. The phonon density of states is then calculated by two machine learning potentials and compared with density functional theory results, with the GAP potential having higher accuracy. Next, the thermal conductivity of a GeTe crystal at 300 K is calculated by the equilibrium molecular dynamics method using both machine learning potentials, and both of them are in good agreement with the experimental results; however, the calculation speed when using the NEP potential is about 500 times faster than when using the GAP potential. Finally, the lattice thermal conductivity in the range of 300 K–600 K is calculated using the NEP potential. The lattice thermal conductivity decreases as the temperature increases due to the phonon anharmonic effect. This study provides a theoretical tool for the study of the thermal conductivity of GeTe.

Keywords: machine learning potentials, thermal conductivity, molecular dynamics

PACS: 74.70.Dd, 74.25.fc, 74.25.Ha, 74.62.–c **DOI:** 10.1088/1674-1056/ad1b42

In recent years, as a result of increasingly prominent issues such as the energy crisis and environmental pollution, research on thermoelectric materials has garnered extensive attention. Specifically, GeTe has been the focus of significant research attention as an important thermoelectric and phase change material. The efficiency of thermoelectric conversion depends on the performance of the thermoelectric material, which is quantified by the thermoelectric figure of merit (ZT). $ZT = \frac{S^2\sigma T}{\kappa_E+\kappa_L}$, where $S^2\sigma$ and T are the power factor and temperature, respectively, and κ is the thermal conductivity, which contains both electronic and lattice components. To enhance the ZT value, it is necessary to increase the power factor while reducing the thermal conductivity. Consequently, the study of thermal conductivity is of great importance, and researchers have dedicated significant efforts to this topic.[1–4]

The advancement of machine learning potential[5,6] has enabled the calculation of lattice thermal conductivity through molecular dynamics (MD) methods. Sosso *et al.*[7] trained the neural network potential of GeTe and conducted calculations of the lattice thermal conductivity of GeTe in its amorphous phase using the equilibrium molecular dynamics (EMD) method. Campi *et al.*[8,9] investigated the impact of Ge vacancy defects on the lattice thermal conductivity of crystalline GeTe using the non-equilibrium molecular dynamics (NEMD) approach. Their findings indicated that a 3% vacancy rate led to a reduction in the thermal conductivity from 3.2 $W\cdot m^{-1}\cdot K^{-1}$ to 1.38 $W\cdot m^{-1}\cdot K^{-1}$. Ghosh *et al.*[10] conducted a study on the lattice thermal conductivity of GeTe films across a temperature range from room temperature to 500 K. Their findings revealed a notable disparity in the contribution of the film compared to the interface thermal resistance between the film and the upper and lower layers.

Recently, Dorde *et al.*[11] trained a Gaussian approximation potential (GAP) and used it to study the temperature evolution of GeTe lattices, demonstrating excellent performance. However, the neuro-evolution potential (NEP), which is based on a separable natural evolution strategy, may have a great advantage in computational speed.[12–14] In order to conduct a comparative study of the GAP and NEP potentials, in this work, we first train a NEP based on the dataset constructed by *ab initio* molecular dynamics (AIMD) calculations. Next, the computational accuracy and computational speed of the two potentials are compared by calculating the phonon density of states and the thermal conductivity of GeTe crystals at 300 K. Finally, the thermal conductivity of GeTe crystals in the range of 300 K–600 K is calculated by the NEP. This study provides a theoretical tool for the study of the thermal conductivity of GeTe.

The GeTe crystal exhibits both rhombohedral and cubic phases, with the rhombohedral phase being dominant at room temperature.[11] The primitive unit cell (UC) used in this paper is shown in Fig. 1. Dorde *et al.*[15] have employed the

†Corresponding author. E-mail: hczhang@hit.edu.cn
‡Corresponding author. E-mail: zhangg@ihpc.a-star.edu.sg

© 2024 Chinese Physical Society and IOP Publishing Ltd

AIMD method to construct a training set, which contains a total of 148 structures in supercells of varying sizes (128–512 atoms) and temperatures (primarily below 800 K, with a few at 1500 K). Additionally, this training set has been used by Dorde *et al.*[11] to train the GAP potential. In this paper, we also train the NEP potential with this training set. The cutoff value is the most crucial parameter in the training process of NEP using GPUMD,[16,17] as it significantly affects the computational speed. The cutoff value is comprised of two parameters: the radial cutoff and the angular cutoff. The radial cutoff is set at 6.5 Å, consistent with the GAP potential, while the angular cutoff is also established at 6.5 Å. The remaining parameters are selected as default settings. A total of 1500 generations are trained, with each generation containing 100 steps. The training process loss function is shown in Fig. 2(a). As the number of fitting generations increases, the loss functions of energy and force decrease and converge. Conversely, the magnitude of the weight (L1) and deviation (L2) parameters in the neural network first increases and then decreases, which can effectively solve the overfitting phenomenon. Figures 2(b) and 2(c) show the energy and force calculated by the NEP potential versus density functional theory (DFT), respectively. The distribution of both energy and force is diagonal, indicating the precision of the NEP potential.

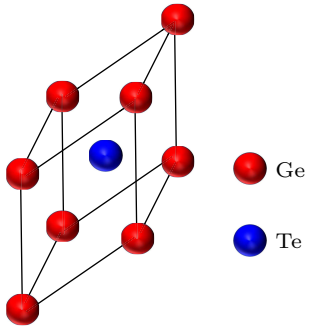


Fig. 1. The primitive unit cell of the rhombohedral GeTe.

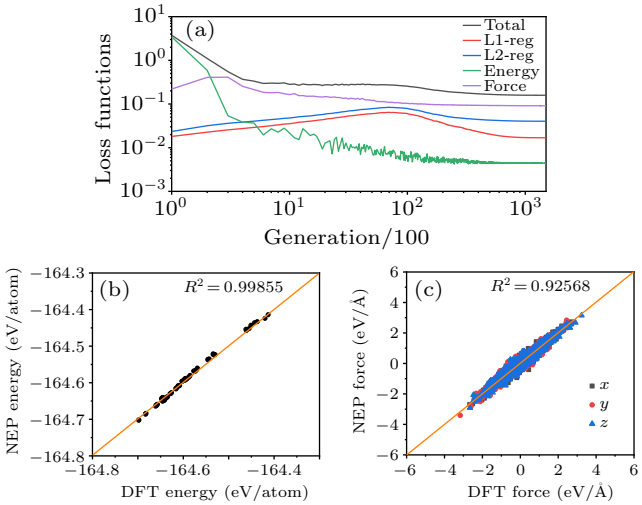


Fig. 2. (a) The evolution of the loss functions (total, L1, L2, energy, and force) during the training process. (b) The energy calculated by NEP versus DFT. (c) The force calculated by NEP versus DFT.

We further use the phonopy tool[18,19] to calculate the phonon density of states by the GAP and NEP potentials. The result of DFT calculations[11] is selected as a reference. The supercells used in our calculations are $8 \times 8 \times 8$ UC, and the calculation results are shown in Fig. 3. Compared with the NEP potential, the GAP potential has higher accuracy.

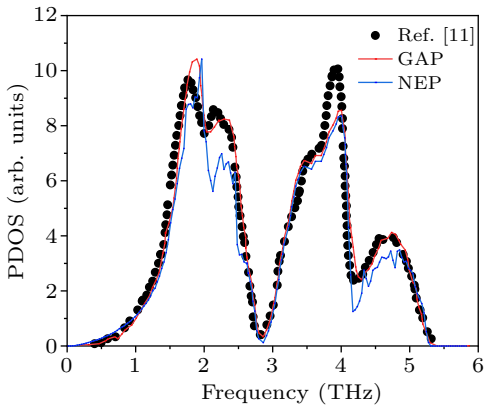


Fig. 3. The phonon density of states of GeTe with the GAP and NEP potentials, and the results of DFT calculations as a reference.[11]

We calculate the lattice thermal conductivity of the rhombohedral GeTe using the NEP potential trained in this work and the GAP potential trained by Dorde *et al.*[11] for comparison. We use the LAMMPS packages[20] to calculate the lattice thermal conductivity by the EMD method, which calculates the lattice thermal conductivity by integrating the heat current autocorrelation function (HCACF) based on the Green–Kubo formula[21,22]

$$\kappa = \frac{1}{3k_{\mathrm{B}}T^2V}\int_0^{\infty} \mathrm{d}t \left\langle \boldsymbol{J}(0)\cdot\boldsymbol{J}(t)\right\rangle, \tag{1}$$

where k_{B} is the Boltzmann constant, V is volume, T is temperature, $\boldsymbol{J}$ is the heat current, and the angular bracket is averaged over the ensemble. In theory, when the integration time approaches infinity, the method exhibits no computational error.[23] In practice, the computing time is always finite, which inevitably introduces numerical errors;[24] therefore, a reasonable cutoff is needed. Two methods can be used to determine the cutoff time: first dip (FD)[25] and first avalanche (FA).[24] The FD method sets the cutoff time at the moment when the HCACF decays to zero for the first time, whereas the FA method sets the cutoff time at the moment when there is a sudden increase and a jump in $F(t)$, which is defined as

$$F(t) = \left|\frac{\sigma(\mathrm{Cor}(t))}{E(\mathrm{Cor}(t))}\right|, \tag{2}$$

where σ and E are the standard deviation and mean of the HCACF over a short time period. The FA method is effective when dealing with thermal conductivity without converging plateau values.[26] Therefore, in this paper, we use the FA method.

In order to use the GAP and NEP potentials in LAMMPS, we compile the QUIP[27] and NEP-LAMMPS,[14] respectively. During the simulation, a GeTe unit cell is used as the basic unit, and the supercell contains ($N \times N \times N$) unit cells. Periodic boundary conditions are enforced in all three directions, and the timestep is 1 fs. Before the simulation starts, energy minimization is first conducted. Subsequently, all atoms are given an initial velocity corresponding to 300 K with the Gaussian distribution. Next, the system is placed in the canonical (NVT) ensemble for 50 ps to fully relax. Finally, the system is placed in the micro-canonical (NVE) ensemble. We perform heat current autocorrelation every 40 ps, for a total of 10 times, and the typical average heat current autocorrelation in a $10 \times 10 \times 10$ supercell (other simulations are similar) is shown in Fig. 4(a). The HCACF decays first rapidly and then slowly to 0. And with $N = 10$, the HCACF can still decay to approximately 0 within 40 ps, which shows that the total simulation time is enough in this study. Moreover, we further calculate the $F(t)$, as shown in Fig. 4(b), and select the moment when $F(t)$ increased to 1 as the cutoff time. To ensure the calculation accuracy, we calculate the cutoff time of different supercells. Figure 4(c) shows the results of the lattice thermal conductivity with different supercells by GAP and NEP. The ultimate result is an average of 10 realizations. When N is less than 6, there is a finite size effect on the thermal conductivity due to periodic boundaries.[28,29] When N is more than 6, the calculated values converge to constants, which can be regarded as the lattice thermal conductivity of the bulk system. The lattice thermal conductivities calculated by the GAP and NEP potentials are (2.45 ± 0.30) W·m^{-1}·K^{-1} and (2.84 ± 0.30) W·m^{-1}·K^{-1}, respectively, which is in good agreement with the experimental data, (2.5–3.6) W·m^{-1}·K^{-1}.[30–32] This is due to the machine learning potentials being trained using the dataset constructed from AIMD calculations, which accurately describes the potential energy surface (PES) and interpolates the results of the DFT calculations. In addition, the MD simulations include all orders of lattice anharmonicity and phonon scattering. The results in this paper are also applicable to other systems, such as 2D Si and bulk PbTe,[12] demonstrating the applicability of the NEP potential in heat transfer calculations.

We first calculate the thermal conductivity by the GAP potential; however, when we further use the NEP potential, the computing platforms are updated. Therefore, we have to choose the computing platforms with the closest parameters for comparison: GAP (Intel Xeon 8360H 48-core 3.0 GHz) and NEP (Intel 8268 48-core 2.9 GHz). The computing time of the different supercell sizes is shown in Fig. 5. As the supercell increases, the GAP potential's computing time increases significantly. When $N = 10$, the computing time reaches 1200 hours (with 96 cores). On the other hand, the calculation using NEP is much faster. For $N = 10$, the computing time using NEP is only 1.85 hours (with 96 cores), which is less than 0.2% of that using GAP. Unlike the GAP potential based on the Gaussian process regression method, the NEP potential employs a feed-forward neural network model and a separable natural evolution strategy, which results in a significant increase in the computational speed of the NEP potential, as evidenced by the related study on PbTe.[12] Considering its high accuracy in thermal conductivity prediction, as well as its fast computing speed, NEP is preferred in the study of lattice thermal conductivity. Next, we use the NEP potential to calculate the lattice thermal conductivity of GeTe in the temperature range of 300 K–600 K.

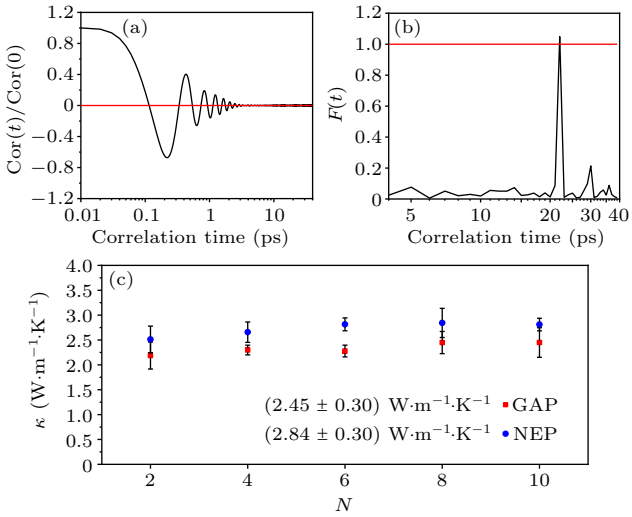


Fig. 4. (a) The normalized HCACF in the $10 \times 10 \times 10$ supercell (other simulations are similar). (b) The $F(t)$ in the $10 \times 10 \times 10$ supercell (other simulations are similar). (c) The lattice thermal conductivity versus supercell size ($N \times N \times N$ unit cells).

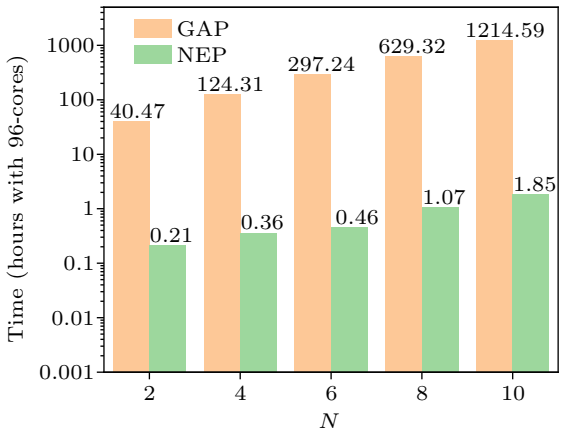


Fig. 5. The computing time of the GAP and NEP potentials in thermal conductivity calculation.

The temperature-dependent lattice thermal conductivity calculated by the NEP potential is shown in Fig. 6. As the temperature rises, the anharmonic effect also increases, leading to a greater influence on lattice thermal conductivity.[33,34] The decrease in thermal conductivity with increasing temperature agrees well with the experimental report[30–32] and the results of the Boltzmann transport approach.[11] It shows that the NEP

potential can capture the anharmonic phonon characteristics of GeTe crystal. This is due to the ability of the NEP potential to accurately predict the PES, which further accurately describes the harmonic and anharmonic force constants, ultimately making its computational accuracy comparable to that of the DFT calculations and enabling it to efficiently predict the thermal conductivity of GeTe crystal.

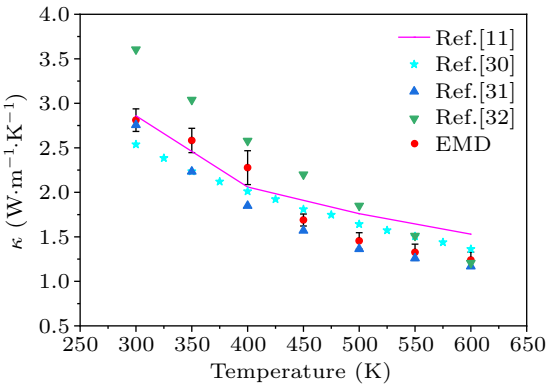


Fig. 6. The lattice thermal conductivity at 300 K–600 K calculated by NEP. The data points reported in Ref. [11] are BTE calculated results, and those in Refs. [30–32] are experimental measurement results.

In summary, we train a NEP using a dataset constructed by AIMD calculations, and the GAP potential is used as a reference. The phonon density of states of different machine learning potentials is first calculated and compared to the DFT calculations, with the GAP potential being more accurate. Next, the thermal conductivity of GeTe crystals at 300 K is calculated by the NEP and GAP potentials using the equilibrium molecular dynamics method, and the results are all in agreement with the experimental results. However, the calculations using the NEP potential are about 500 times faster than those using GAP. Finally, the lattice thermal conductivity in the range of 300 K–600 K is calculated using the NEP potential. The lattice thermal conductivity decreases as temperature increases due to the phonon anharmonic effect. This study provides a theoretical tool for the study of the thermal conductivity of GeTe.

Acknowledgments

Project supported by the A*STAR Computational Resource Centre through the use of its high-performance computing facilities. J. Zhang gratefully acknowledges financial support from the China Scholarship Council (Grant No. 202206120136) and is grateful to Prof. Dorde Dangic for his guidance on the use of GAP.

References

[1] Li X G, Chen J, Yu C X and Zhang G 2013 *Appl. Phys. Lett.* **103** 013111
[2] Li D F, He J, Ding G Q, Tang Q Q, Ying Y, He J J, Zhong C Y, Liu Y, Feng C B, Sun Q L, Zhou H B, Zhou P and Zhang G 2018 *Adv. Funct. Mater.* **28** 1801685
[3] Chen J, He J, Pan D K, Wang X T, Yang N, Zhu J J, Yang S Y A and Zhang G 2022 *Sci. China-Phys. Mech. Astron.* **65** 117002
[4] Zhang Z W and Chen J 2018 *Chin. Phys. B* **27** 035101
[5] Ouyang Y L, Zhang Z W, Yu C Q, He J, Yan G and Chen J 2020 *Chin. Phys. Lett.* **37** 126301
[6] Ouyang Y L, Yu C Q, Yan G and Chen J 2021 *Front. Phys.* **16** 1
[7] Sosso G C, Miceli G, Caravati S, Behler J and Bernasconi M 2012 *Phys. Rev. B* **85** 174103
[8] Campi D, Donadio D, Sosso G C, Behler J and Bernasconi1 M 2015 *J. Appl. Phys.* **117** 015304
[9] Campi D, Paulatto L, Fugallo G, Mauri F and Bernasconi M 2017 *Phys. Rev. B* **95** 024311
[10] Ghosh K, Kusiak A, Noe P, Cyrille M C and Battaglia J L 2020 *Phys. Rev. B* **101** 214305
[11] Dangic D, Hellman O, Fahy S and Savic I 2021 *npj Comput. Mater.* **7** 57
[12] Fan Z Y, Zeng Z Z, Zhang C Z, Wang Y Z, Song K K, Dong H K, Chen Y and Nissila T A 2021 *Phys. Rev. B* **104** 104309
[13] Fan Z Y 2022 *J. Phys. Condens. Matter* **34** 125902
[14] Fan Z Y, Wang Y Z, Ying P H, Song K K, Wang J J, Wang Y, Zeng Z Z, Xu K, Lindgren E, Rahm J M, Gabourie A J, Liu J H, Dong H K, Wu J Y, Chen Y, Zhong Z, Sun J, Erhart P, Su Y J and Nissila T A 2022 *J. Chem. Phys.* **157** 114801
[15] Dangic D, Fahy S and Savic I 2021 *Materials Cloud Archive* 2021.42
[16] Fan Z Y, Siro T and Harju A 2013 *Comput. Phys. Commun.* **184** 1414
[17] Fan Z Y, Chen W, Vierimaa V and Harju A 2017 *Comput. Phys. Commun.* **218** 10
[18] Togo A and Tanaka I 2015 *Scr. Mater.* **108** 1
[19] Togo A 2023 *J. Phys. Soc. Jpn.* **92** 012001
[20] Plimpton S 1995 *J. Comput. Phys.* **117** 1
[21] Green M S 1954 *J. Chem. Phys.* **22** 398
[22] Kubo R 1957 *J. Phys. Soc. Jpn.* **12** 570
[23] Kubo R, Yokota M and Nakajima S 1957 *J. Phys. Soc. Jpn.* **12** 1203
[24] Chen J, Zhang G and Li B W 2010 *Phys. Lett. A* **374** 2392
[25] Li J, Porter L and Yip S 1998 *J. Nucl. Mater.* **255** 139
[26] McGaughey A J H and Kaviany M 2006 *Adv. Heat Transf.* **39** 169
[27] Csanyi G, Winfield S, Kermode J R, DeVita A, Comisso A, Bernstein N and Payne M C 2007 *IoP Comput. Phys. Newsletter* Spring 2007
[28] Che J, Cagin T, Deng W and Goddard W A 2000 *J. Chem. Phys.* **113** 6888
[29] Schelling P K, Phillpot S R and Keblinski P 2002 *Phys. Rev. B* **65** 144306
[30] Li J, Chen Z W, Zhang X Y, Yu H L, Wu Z H, Xie H Q, Chen Y and Pei Y Z 2017 *Adv. Sci.* **4** 1700341
[31] Xing T, Song Q F, Qiu P F, Zhang Q H, Xia X G, Liao J C, Liu R H, Huang H, Yang J, Bai S Q, Ren D D, Shi X and Chen L D 2019 *Natl. Sci. Rev.* **6** 944
[32] Cai S T, Hao S Q, Luo Z Z, Li X, Hadar I, Bailey T P, Hu X B, Uher C, Hu Y Y, Wolverton C, Dravid V P and Kanatzidis M G 2020 *J. Mater. Chem. A* **8** 1193
[33] Yang X L, Tiwari J and Feng T L 2022 *Mater. Today Phys.* **24** 100689
[34] Zhu X Y and Shao C 2022 *Phys. Rev. B* **106** 014305